

# REPORT DOCUMENTATION PAGE

AFRL-SR-BL-TR-99-

38

Public reporting burden for this collection of information is estimated to average 1 hour per response, including maintaining the data needed, and completing and reviewing this collection of information. Send comments to: Washington Headquarters Services, Directorate for Information Operations and Reports, 1204, Arlington, VA 22202-4302, and to the Office of Management and Budget, Paperwork Reduction Project (0704-0188).

0002

es. gathering and  
of information,  
1204, Arlington,

1. AGENCY USE ONLY (Leave blank)		2. REPORT DATE December 31, 1998	3. REPL Final Technical Report, 1/1/96-12/31/98
4. TITLE AND SUBTITLE  Laboratory Studies of the Stratospheric Effects of Rocket Exhaust			5. FUNDING NUMBERS  F49620-96-1-0034  2303/ES 01102F
6. AUTHOR(S)  M.J. Molina, M. Haider, Y. Mantz, L. Gutzwiller and L.T. Molina			8. PERFORMING ORGANIZATION REPORT NUMBER
7. PERFORMING ORGANIZATION NAME(S) AND ADDRESS(ES)  Massachusetts Institute of Technology 77 Massachusetts Avenue Cambridge, MA 02139			10. SPONSORING / MONITORING AGENCY REPORT NUMBER
9. SPONSORING / MONITORING AGENCY NAME(S) AND ADDRESS(ES)  Air Force Office of Scientific Research Directorate of Chemistry and Life Sciences AFOSR/NL, 801 North Randolph Street, Room 732 Arlington, VA 22203-1977			
11. SUPPLEMENTARY NOTES			
12a. DISTRIBUTION / AVAILABILITY STATEMENT  Approved for public release; distribution unlimited			12b. DISTRIBUTION CODE
13. ABSTRACT (Maximum 200 Words)  The most important chlorine activation reaction that takes place in the stratosphere is the heterogeneous reaction of chlorine nitrate with hydrogen chloride to produce molecular chlorine and nitric acid. The reaction is catalytic, promoted by surfaces that are not themselves affected by the reaction. This process was investigated in the laboratory: the reaction probability was found to have a value of about 0.02 on glass, on laboratory alumina, and on alumina particles emitted by solid rocket motors. The reaction probability on ice surfaces has a value larger than 0.2 and a negligible value on halocarbon wax or Teflon surfaces. The measurements were carried out under reactant partial pressure, temperature and humidity conditions covering those that are encountered in the mid-latitude lower stratosphere. The reaction mechanism appears to be determined by the water layers adsorbed on the solid surface. Measurements of the amount of water taken up by alumina surfaces were also carried out; the results indicate that under stratospheric conditions several water layers will indeed cover the alumina surfaces.			
14. SUBJECT TERMS  Stratospheric ozone, Solid rocket motors, Chlorine activation, Mass spectrometry			15. NUMBER OF PAGES 26
			16. PRICE CODE
17. SECURITY CLASSIFICATION OF REPORT UNCLASSIFIED	18. SECURITY CLASSIFICATION OF THIS PAGE UNCLASSIFIED	19. SECURITY CLASSIFICATION OF ABSTRACT UNCLASSIFIED	20. LIMITATION OF ABSTRACT

**Final Technical Report**

**LABORATORY STUDIES OF THE  
STRATOSPHERIC EFFECTS OF ROCKET EXHAUST**

**Prepared for:**

Air Force Office of Scientific Research  
Attention: Dr. Michael R. Berman, Program Manager  
Directorate of Chemistry and Life Sciences  
AFOSR/NL  
801 North Randolph Street, Room 732  
Arlington, VA 22203-1977  
Tel: 703-696-7781

**AFOSR Grant Number:**

F49620-96-1-0034

**Principal Investigator:**

Mario J. Molina,  
Massachusetts Institute of Technology  
77 Massachusetts Avenue, Bldg. 54-1814  
Cambridge, MA 02139  
Phone: 617-253-5081; Fax: 617-258-6525  
E-mail: mmolina@MIT.EDU

December, 1998

19990125 052

## CONTENTS

Introduction .....	1
Experimental Section .....	5
A. Reaction Probability Measurements .....	5
B. Sampling of SRM Emission Dust .....	9
C. Characterization of Alumina Particles .....	9
D. Uptake of Water Vapor by Alumina Particles .....	10
Results and Discussion .....	13
A. Chemical Kinetics Experiments .....	13
B. Uptake of Water Vapor by Alumina and Sapphire Particles.....	16
Conclusions .....	22
Acknowledgment .....	22
References .....	23
Appendix .....	24

# Laboratory Studies of the Stratospheric Effects of Rocket Exhaust

## INTRODUCTION

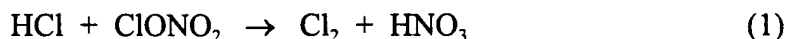
The Space Shuttle, as well as Titan III and Titan IV rockets, are propelled by solid rocket motors (SRMs) containing aluminum (Al) and sodium perchlorate ( $\text{NaClO}_4$ ). One third of the emissions -mostly aluminum oxide particles (alumina,  $\text{Al}_2\text{O}_3$ ), hydrogen chloride (HCl) and water- are deposited in the stratosphere up to an altitude of 43 km (~112 ton alumina / launch) [Brady *et al.*, 1997]. Alumina particles emitted by SRM's have been collected and characterized previously [Cofer *et al.*, 1989; Beiting, 1995]. They appear to be spherical, exist in the cubic- $\gamma$  and hexagonal- $\alpha$  phases, and contain trace amounts of K, Na, Ti, Fe and Si as well as surface contamination of chlorides and oxychlorides.

There have been several investigations of the potential stratospheric effects of such emissions, focussing primarily on ozone depletion in the vicinity of the rocket plume [see, e.g., Prather *et al.*, 1990; Denison *et al.*, 1994; Jones *et al.*, 1995; Ross *et al.*, 1997a, b]. Global effects have also been considered [e.g., WMO, 1995], but have received somewhat less attention. The reductions on stratospheric ozone induced by chlorine compounds released by SRMs should be practically the same as those of chlorine released by the decomposition of industrial chlorofluorocarbons (CFCs), if the altitude and the magnitude of the injection is taken into account. The reason is that the various inorganic forms of stratospheric chlorine inter-convert to each other on a time scale that is short compared to diffusion out of the stratosphere. The dominant effect of the injection altitude is the residence time of the emissions, which is of the order of several years for injections at mid-stratospheric altitudes. There are, of course, also latitudinal and seasonal effects, but these are in general less pronounced.

A separate atmospheric effect from SRM emissions is that resulting from the alumina particles. These can potentially enhance nucleation, or promote surface chemical reactions that might influence the ozone balance in the stratosphere. There are reports from measurements in the stratosphere suggesting that the concentration of

aluminum-containing particles increased very significantly during the 1970's and early 1980's [Brownlee *et al.*, 1976; Zolensky *et al.*, 1989]; this increase was attributed in part to Space Shuttle launches, but predominantly to ablating spacecraft material.

Surface reactions leading to chlorine activation are well documented for stratospheric aerosols at high latitudes; such heterogeneous reactions play a key role in polar ozone depletion. Chlorine activation is the process converting relatively stable reservoir species to active ones, which decompose readily by the action of solar radiation to yield catalytically active free radicals. The most important chlorine activation reaction is the following:



At low latitudes stratospheric aerosols consist predominately of concentrated sulfuric acid solutions (>70 % weight). Chlorine activation does not occur efficiently on these aerosols because of the very low solubility of HCl in such concentrated acid solutions. At higher latitudes, with correspondingly lower temperatures, the sulfuric acid aerosols become more dilute, and eventually form polar stratospheric clouds, consisting of ice or of various solid acid hydrates; it is on the surfaces of such aerosols that reaction (1) occurs with high probability [Molina *et al.*, 1987]. This is a catalytic process in the sense that the aerosol surface participates in the chemical reaction, but is regenerated after each reaction cycle, i.e. a large number of gas phase molecules are processed by the surface. Species such as HCl and HNO<sub>3</sub> do not accumulate in the particles, and are essentially at equilibrium in terms of physical partitioning between the gas and the condensed phase. On the other hand, aluminum oxide particles from SRMs can in principle catalyze chlorine activation even at low latitudes. If that is the case, the global effects of such particles on stratospheric ozone could very well be as significant as the effects of chlorine emissions from SRMs.

Recently, we investigated the reaction probability  $\gamma$  of HCl + ClONO<sub>2</sub> on Pyrex glass and on a proxy for the particulate SRM emissions,  $\alpha$ -alumina, under stratospheric conditions using a low-pressure flow-tube (~3 cm I.D., 35 cm long) interfaced to a

quadrupole mass spectrometer. The reaction probability  $\gamma$  is defined as the ratio of the number of collisions that lead to reaction to the total number of collisions with the surface. In the first set of experiments, we inserted a 1.6-cm I.D. alumina tube (Omega Engineering) into the glass flow-tube. In the second set, we placed non-porous  $\alpha$ -alumina particles with an average diameter of  $\sim 3$   $\mu\text{m}$  in a Teflon boat located inside the flow-tube. Under quasi-stratospheric conditions, pseudo-first order rate constants were determined from chlorine ( $\text{Cl}_2$ ) growth or chlorine nitrate ( $\text{ClONO}_2$ ) decay curves, using electron impact mass spectrometry and chemical ionization mass spectrometry (CIMS). Our results indicate that  $\gamma$  has a value of  $\sim 0.02$ , independent of temperature between 190 and 230 K. This value decreases significantly when the reaction is carried out on "dry surfaces," following accumulation of the product  $\text{HNO}_3$  on the alumina surface. After replenishing the water on the alumina surface, a  $\gamma$  value of 0.02 could be re-established. This, and the fact that the same  $\gamma$  was determined on Pyrex glass, implies that the mechanism of the reaction depends not on the detailed nature of the oxide surface itself, but rather on the presence of water layers adsorbed on the surface. These experiments have been described and published in the literature [Molina *et al.*, 1997].

Jackman *et al.* [1998] used our measured  $\gamma$  value of 0.02 to estimate the global impact of SRM emissions on stratospheric ozone using the Goddard Space Flight Center two-dimensional photochemistry and transport model. Utilizing a historic launch scenario from 1970-1997, they calculated an annually averaged global total ozone loss of 0.025 % for 1997 in an alumina and HCl perturbed stratosphere. Alumina is responsible for approximately one third, whereas hydrogen chloride as part of the SRM emissions contributes about two thirds of this loss (0.025 %).

As mentioned above, chlorides and oxychlorides were found on the surface of the particulate emissions as contaminants; this is an indication that the surfaces of clean laboratory alumina and Space Shuttle dust might have different chemical reactivities. Hence, the reaction probability for reaction (1) might be dissimilar. Therefore, we carried out additional experiments using authentic SRM dust emissions.

In order to further test the hypothesis that the reaction mechanism for the chlorine activation process is determined by the water layers adsorbed on the alumina particles,

we also investigated the uptake of water vapor by two types of  $\alpha$ -alumina surfaces: sapphire and conventional alumina.

In the experimental section we describe the flow tube-chemical ionization mass spectrometer apparatus designed to operate with a miniature flow tube, in order to enable measurements with very small amounts of alumina samples. We also describe the apparatus employed for the water uptake experiments. In a subsequent section we report the results of our measurements of the chlorine activation reaction on Pyrex glass, micron sized  $\alpha$ -alumina, SRM particle emissions and SRM slack under temperature, humidity and reactant partial pressure conditions similar to those prevailing in the lower stratosphere at mid-latitudes. We also describe in that section the results of our water uptake experiments.

## EXPERIMENTAL SECTION

### A. Reaction Probability Measurements

A schematic of the experimental apparatus is shown in Figure 1. It consists of a flow-tube (~ 4mm I.D. and 15 cm long) interfaced to a chemical ionization quadrupole mass spectrometer (ABB Extrel). The alumina samples were deposited on the inside walls of the flow-tubes. The tube walls had been previously coated with halocarbon wax (Halocarbon Product Inc.). After particle deposition, the glass tube was observed with an optical microscope (Axioskop 20, Zeiss) in order to assess the concentration of the particles on the tube walls.

ClONO<sub>2</sub> was injected through a movable injector (stainless steel tubing, 1/16" O.D.) while a diluted mixture of HCl (0.09% in N<sub>2</sub>, Matheson) in He was mixed upstream with additional He (UHP Grade) carrier gas. The injector was centrally aligned to prevent removal of the particles deposited on the flowtube walls while sliding the injector back and forth. ClONO<sub>2</sub> was synthesized [Molina *et al.*, 1977] and prepared in a bulb at a mixing ratio of 10<sup>-3</sup>. The ClONO<sub>2</sub> / He from the bulb was subsequently diluted with additional He and split injected into the He carrier gas stream (split ratio is typically 1:100). As long as the pressure in the mixing tube is higher than one atmosphere and the excess flow is substantial (> 10 sccm), back diffusion of ambient air into the system is negligible.

The flowtube was inserted in a cooling stage machined from an aluminum block with boreholes for three heating cartridges (100 watt) and for two thermocouples. The temperature was controlled by constant cooling provided by a liquid nitrogen reservoir and counterbalanced by the resistive heaters coupled to a temperature controller. The temperature was measured with two copper-constantan thermocouples.

Using the CIMS approach, we were able to achieve a high detection sensitivity for ClONO<sub>2</sub> and Cl<sub>2</sub> with a linear detector response between 10<sup>9</sup> and 5x10<sup>10</sup> molecule/cm<sup>3</sup> (3x10<sup>-8</sup> - 1.5x10<sup>-6</sup> Torr.). The negative reagent ion, SF<sub>6</sub><sup>-</sup>, was generated by passing neutral SF<sub>6</sub> in a flow of nitrogen through a radioactive polonium ion source (<sup>210</sup>Po, Model P2031, NRD Inc.). The lowest practical N<sub>2</sub> flow in this system was 375 sccm. Apart

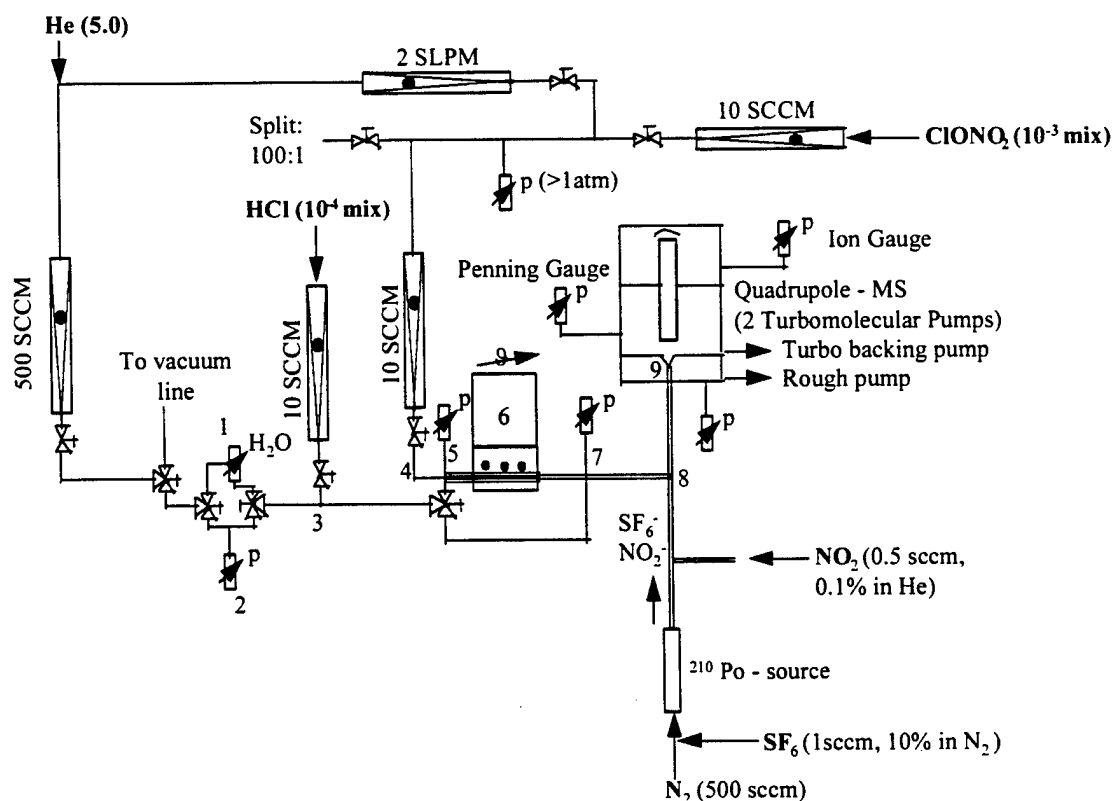


**Figure 1:** Schematic representation of the flowtube—chemical ionization mass spectrometer apparatus. All tubing consists of 1/8" stainless steel up to point labeled 5; beyond, it consists of 1/4" glass tubing. 1: Dew point measurement; 2: Pressure measurement to determine the humidity in the reaction zone; 3: HCl injection into He carrier gas; 4: Injection of ClONO<sub>2</sub> through a movable stainless steel 1/16" injector; 5: Pre-flowtube pressure measurement; 6: Cooler; 7: Post-flowtube pressure measurement; 8: Ionization of reactants and products; 9: Ion extraction through a 0.5 mm orifice biased at -105 V.

from the higher pressure (typically 1 - 10 Torr) in the ionization region, a better mixing leads to an increase in sensitivity for reactants and products.  $\text{ClONO}_2$ ,  $\text{HCl}$  and  $\text{Cl}_2$  were detected as  $\text{FClONO}_2^-$  (116 amu),  $\text{SF}_5\text{Cl}^-$  (162 amu) and  $\text{Cl}_2^-$  (70 amu). In addition,  $\text{NO}_2$  was injected downstream of the polonium source. Using He carrier gas (UHP Grade), the water vapor partial pressure in the flowtube was of the order of  $10^{-4}$  Torr so that the experiments were conducted under quasi-stratospheric conditions of humidity. Table 1 summarizes the relevant experimental parameters.

As part of this project we also developed an improved interface between the chemical ionization reactor and the mass spectrometer vacuum chamber [Zhang *et al.*, 1998]. This interface consists of an electrostatic ion guide that enables high-speed pumping of the neutral molecules while efficiently channeling the ions into the quadrupole mass analyzer. A more detailed description of this ion guide is presented as an Appendix.

The  $\text{HCl}$  concentration was at least in fivefold and typically in tenfold excess over  $\text{ClONO}_2$  to ensure pseudo-first-order conditions. Typical reagent concentrations were in the range from 3 to  $5 \times 10^{10}$  molecule/ $\text{cm}^3$  ( $1.0$ - $1.6 \times 10^{-6}$  Torr) for  $\text{ClONO}_2$  and  $3 \times 10^{11}$  molecule/ $\text{cm}^3$  ( $10^{-5}$  Torr) for  $\text{HCl}$ , respectively. Other parameters are summarized in Table 1. The reaction probabilities were obtained from the decay of the  $\text{FClONO}_2^-$  signal, monitored while pulling back the injector at 2-cm increments.

Five sets of measurements were conducted at two different temperatures (223 K and 238 K), each at least four times in a row. First, the chlorine activation reaction was investigated on halocarbon wax to determine the reaction probability  $\gamma$  on this support surface; as expected,  $\gamma$  is negligible on this surface compared to the value on glass or alumina. Second, the reaction was investigated on Pyrex glass, in order to verify the  $\gamma$  value of 0.02 obtained earlier [Molina *et al.*, 1997]. Subsequently, the reaction was studied on  $\alpha$ -alumina, on SRM dust and finally on SRM slack. These sets of experiments provided only a relative  $\gamma$  value; a subsequent experiment was conducted with a "capped" injector, designed to inject  $\text{ClONO}_2$  against the flow of He carrier gas, with improved mixing to enable the use of standard flowtube equations with diffusion corrections [Zasytkin *et al.*, 1997].

**Table 1: Parameters for Flowtube—CIMS Experiments**

N <sub>2</sub> make-up gas flow	500 - 750 sccm
SF <sub>6</sub> flow and mixing ratio	1 sccm (10 % in N <sub>2</sub> )
NO <sub>2</sub> flow and mixing ratio	0.5 sccm (0.1 % in N <sub>2</sub> )
He (4.7) carrier gas flow	750 sccm
ClONO <sub>2</sub> mixing ratio in bulb	10 <sup>-3</sup>
HCl mixing ratio in bulb	10 <sup>-4</sup>
Humidity in flowtube	~1.3·10 <sup>-13</sup> molec/cm <sup>3</sup> (~ 4x10 <sup>-4</sup> Torr)
Pressure in flowtube	22 - 30 Torr
Reaction temperature	223 K, 238 K
Maximum reaction distance	10 cm
Pressure in ionization region	1 - 10 Torr
Ionization reaction time	1 - 3 ms
Orifice diameter	0.5 mm
Orifice voltage	- 105 V
ClONO <sub>2</sub> concentration and partial pressure	3 - 5x10 <sup>10</sup> molec/cm <sup>3</sup> (1.0 - 1.6x10 <sup>-6</sup> Torr)
HCl concentration and partial pressure	3x10 <sup>11</sup> molec/cm <sup>3</sup> (10 <sup>-5</sup> Torr)
Limit of Detection (LOD) - ClONO <sub>2</sub>	3x10 <sup>9</sup> molec/cm <sup>3</sup> (10 <sup>-7</sup> Torr)
LOD - HCl	7x10 <sup>9</sup> molec/cm <sup>3</sup> (2x10 <sup>-7</sup> Torr)
LOD - Cl <sub>2</sub> (without NO <sub>2</sub> )	1x10 <sup>10</sup> molec/cm <sup>3</sup> (3x10 <sup>-7</sup> Torr)
LOD - Cl <sub>2</sub> (with NO <sub>2</sub> )	7x10 <sup>9</sup> molec/cm <sup>3</sup> (2x10 <sup>-7</sup> Torr)

### **B. *Sampling of SRM Emission Dust.***

The sample was collected at Thiokol Propulsion Inc., and was provided to us by R.R. Bennett. It was obtained from several static test firings of small rocket motors containing SRM propellant. The collection of this material proved to be quite difficult, because the particles are very small and buoyant. The sample was obtained by igniting each time roughly 150 g of propellant in a small rocket motor and expanding the plume out of a graphite nozzle into an 8-inch diameter sheet metal tube. The tube was 5 feet long and opened into a 30-gallon barrel. The center of the lid of the barrel had previously been removed and another 8-inch diameter and 6-feet long metal tube had been inserted. The end of the tube extended about two feet into the barrel. This setup was chosen in order to cause sufficient turbulence to be able to sample the SRM dust from the walls of the barrel and the tubes. The exhaust flow was so high and the particles were so small that the amount sampled was only about 100 mg. In addition, a sample of SRM slack provided to us by the Aerospace Corporation was ground to yield particles with an equivalent diameter of 1-2  $\mu\text{m}$ .

### **C. *Characterization of the Alumina Particles***

The two types of sample (SRM dust and SRM slack) and different size fractions of reference laboratory  $\alpha$ -alumina (0.88, 2.86 and 10-45  $\mu\text{m}$  average particle size) were examined and compared with an optical microscope. Both samples have a grayish color, most likely due to the presence of some solid aluminum. The majority of the particles of both samples have an average size in the range of 1-2  $\mu\text{m}$ . Therefore, the laboratory  $\alpha$ -alumina with a Fisher size of 0.88  $\mu\text{m}$  (Cerac Inc.) was taken as a proxy for the preparation of the flowtubes. The small SRM dust sample enabled us to coat only one tube, justifying our effort to downsize the flowtube. We prepared three tubes of the slack sample as well as three tubes of the laboratory  $\alpha$ -alumina. HCl breakthrough experiments were conducted in order to estimate the alumina surface area. The results indicate that the SRM alumina samples and reference laboratory  $\alpha$ -alumina have comparable surface areas. The number of particles deposited on the tube walls was roughly of the order of one monolayer of closely packed particles. Breakthrough

experiments on uncoated Pyrex glass and on halocarbon wax-coated tubes were also carried out. For each surface, breakthrough experiments were carried out at least three times at 223 K. The results are listed in Table 2. Complete flow-tube surface coverage by the alumina particles was confirmed using the optical microscope. The SRM dust showed a high HCl background, corresponding to approximately  $10^{-5}$  Torr HCl, confirming that the particles were in contact with the carrier gas and did not become covered with wax during preparation.

#### ***D. Uptake of Water Vapor by Alumina Particles***

A schematic representation of the apparatus that we employed for the water adsorption measurements is shown in Figure 2. It consists of a small diameter column containing the alumina or sapphire particles coupled to a detector for water vapor. The water vapor is monitored by using a microwave plasma to induce emission of Lyman- $\alpha$  radiation by the hydrogen atoms originally present in the water molecules. The radiation intensity is recorded as a function of time by a solar blind photomultiplier (R 1259, Hamamatsu) attached to a vacuum ultraviolet monochromator (Acton Research Corporation). Using a 2-way valve, the pure carrier gas (He) is switched to a gas mixture with a known water partial pressure. The time elapsed between switching the valve and observing the breakthrough of the water through the column is recorded. In a reference experiment, the breakthrough time is measured using  $H_2$  instead of water. The difference in breakthrough time is the actual retention time and is proportional to the amount of water adsorbed by the column. More specifically, the area between the two curves is used to measure the amount of adsorbed water. Typical gas flows are 10 sccm and are measured using commercial flowmeters (Tylan General). The absolute water partial pressure was determined using a moisture probe (Panametrics) with a detection limit corresponding to a dew point of  $-110^\circ\text{C}$  (163.3 K). A frost point of 193.3 K corresponds to 0.4 mTorr water partial pressure, or 5 ppm at a stratospheric pressure of 80 Torr.

We prepared packed columns with two samples:  $\alpha$ -alumina supplied by Cerac, Inc. and sapphire particles, which is a particularly inert form of aluminum oxide. The samples were packed into a quartz tube of 1-mm I.D. For some experiments, the sample

was heated to 1300 K; this annealing process was carried out to remove hydroxyl groups from the alumina surface.

**Table 2:** Average surface areas determined by three or more HCl breakthrough experiments for each surface at 223 K (assuming  $10^{15}$  HCl molecule /  $\text{cm}^2$  and geometrical surface area as reference) and average relative reaction probability  $\gamma \pm 2\sigma$ .

Surface	Temperature K	Estimated number of HCl monolayers	Average $\gamma \pm 2\sigma$
Glass (open injector.)	223	0.5	$0.0037 \pm 0.0004$
Glass (open injector.)	238	0.5	$0.0040 \pm 0.0005$
Glass (capped inject.)	228-232	0.5	$0.0155 \pm 0.015$
Halocarbon wax	223	0.3	$0.0021 \pm 0.0007$
Halocarbon wax	238	0.3	$0.0028 \pm 0.0003$
$\alpha$ -alumina (0.88 $\mu\text{m}$ )	223	0.2	$0.0184 \pm 0.0036$
$\alpha$ -alumina (0.88 $\mu\text{m}$ )	238	0.2	$0.0195 \pm 0.0032$
SRM dust ( $\sim 1 \mu\text{m}$ )	223	0.9	$0.0214 \pm 0.0024$
SRM dust ( $\sim 1 \mu\text{m}$ )	238	0.9	$0.0166 \pm 0.0035$
SRM slack ( $\sim 1 \mu\text{m}$ )	223	0.4	$0.0109 \pm 0.0009$
SRM slack ( $\sim 1 \mu\text{m}$ )	238	0.4	$0.0133 \pm 0.0011$

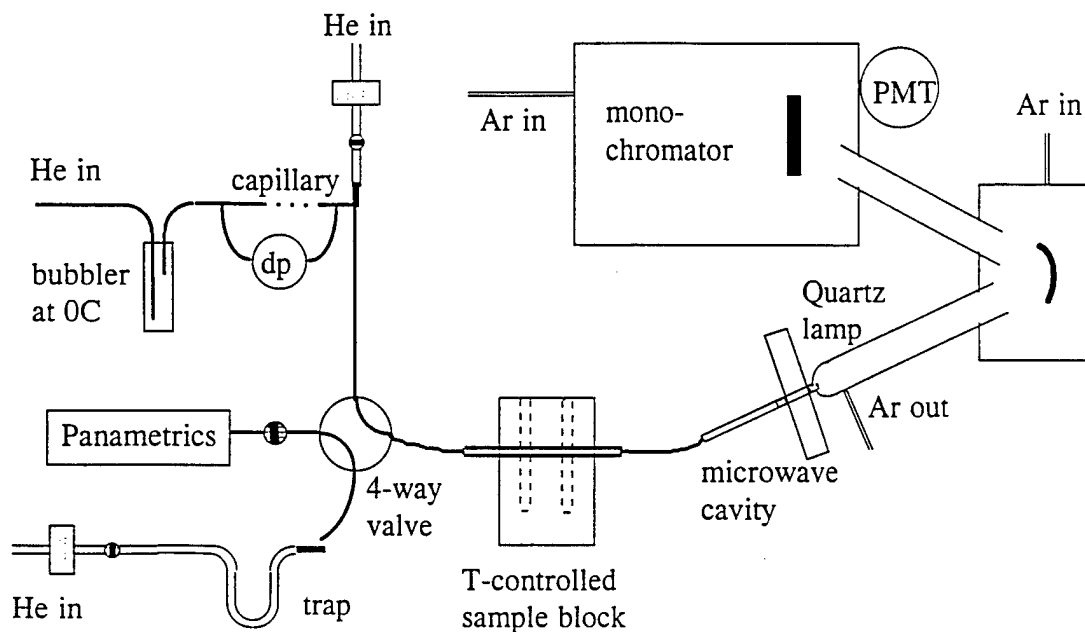


**Figure 2:** Schematic of the apparatus to measure water vapor uptake by alumina particles. The breakthrough curve of water is monitored using the Lyman- $\alpha$  emission of atomic hydrogen. Typical flow of carrier gas (He) is 10 sccm. PMT= photomultiplier tube, dp=differential pressure across capillary.

## RESULTS AND DISCUSSION

### A. Chemical Kinetics Experiments

For every surface about ten reactant decays were determined at each temperature, summing up to approximately 100 experiments. Pseudo-first-order rate constants were calculated from the decays in terms of the ratio of signal at a given reaction length  $x$  to the initial signal at reaction length equal to 0 ( $S_x / S_0$ ). From these pseudo-first-order reaction rate constants  $\gamma$  was computed assuming the law of additivity of kinetic resistances [Zasyupkin *et al.*, 1997]:

$$\frac{1}{k_{\text{obs}}} = \frac{1}{k_d} + \frac{1}{k_w}, \quad (2)$$

where  $k_{\text{obs}}$  stands for the observed pseudo-first-order rate constant,  $k_d$  for the diffusion rate constant and  $k_w$  for the (wall) collision rate constant, all in units of  $\text{s}^{-1}$ . The diffusion rate constant is calculated as follows:

$$k_d = \frac{3.66D_c}{r^2} \quad (3)$$

We employed a value for the diffusion coefficient  $D_c$  for  $\text{ClONO}_2$  in He at 200 K of  $176 \text{ Torr cm}^2 \text{ s}^{-1}$ , estimated assuming a temperature dependence of  $T^{1.76}$  [Hanson and Ravishankara, 1991]. The reaction probability  $\gamma$  was then calculated as follows:

$$\gamma = \frac{2rk_w}{\omega + rk_w} \quad (4)$$

In equations 3 and 4,  $r$  stands for the radius of the flow-tube in cm, and  $\omega$  is the mean thermal velocity in cm/s. The results are shown in Table 2 and are plotted in Figure 3. The standard deviations for the  $\gamma$ 's were obtained by propagating the standard

deviations of the observed pseudo-first-order rate constants  $k_{\text{obs}}$ . Most of the regression coefficients of the  $k_{\text{obs}}$  fits were larger than 0.97.

The blank test on a tube covered only with halocarbon wax exhibited only a small reaction probability for the chlorine activation reaction; halocarbon wax can therefore be considered as a suitable support for the alumina particles at least down to 223K.

The reaction probabilities reported in Figure 3 and Table 2 represent only relative values. The reason is that equations 2-4 are not strictly valid for our system; the flow dynamics and reactant mixing length is not sufficiently well characterized to enable absolute calculations of the diffusion corrections. The complication arises in part from the use of a straight open injector: mixing of the reactant plume at the operating pressure of ~25 Torr is relatively slow under these conditions, whereas equations 2-4 assume perfect mixing. Furthermore, the flow-tube has a porous particle layer with a complicated geometry that slows down diffusion of the reactant to the solid surface; equation 2 assumes a smooth cylindrical flow-tube surface. Although it is possible to estimate the magnitude of the required correction factors (see, e.g., Keyser *et al.*, 1991), this cannot be done with sufficient accuracy. Nevertheless, the measured decay rate constants and the use of equations 2-4 do provide reasonably accurate relative values for the reaction probabilities. The results show very clearly that the  $\gamma$ 's have essentially the same value on all the alumina samples –SRM dust, SRM slack, and laboratory  $\alpha$ -alumina. Our earlier experiments had already indicated that the reaction probability is the same on glass and on alumina. As described in the introduction, based on the assumption that the reaction mechanism is determined by the presence of a water bilayer adsorbed on the surface, these are the expected results.

In order to directly compare the small-bore flow-tube results described above with those of our earlier experiments conducted with a conventional flow-tube, we carried out a control experiment designed to yield an absolute reaction probability value. For this purpose we employed a smooth Pyrex glass flow-tube surface and we modified the injector by placing a cap at its outlet in order to achieve rapid mixing. As indicated in Table 2 and Figure 3, the results of this control experiment indicate that the  $\gamma$  value on

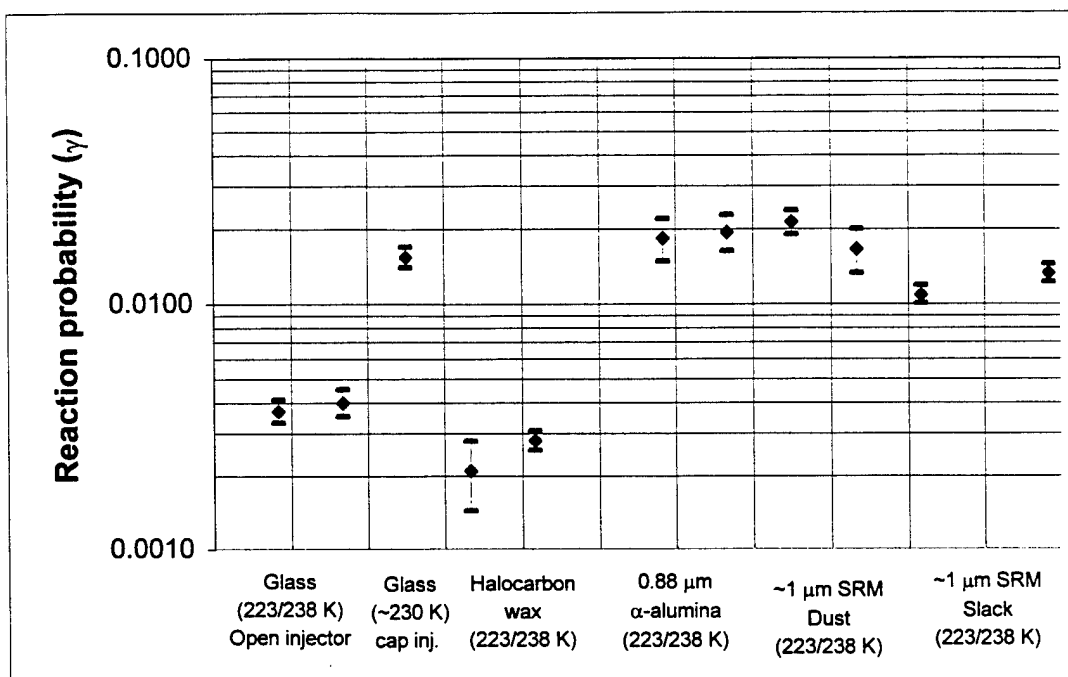


**Figure 3:** Experimentally determined relative reaction probabilities ( $\gamma \pm 2\sigma$ ) for the chlorine activation reaction on the indicated surfaces. The left data point for each distinct surface corresponds to the average of measurements carried out at 223 K, the right data point at 238 K, respectively. The averaged  $\gamma$ 's as well as the standard deviations  $\sigma$  are derived from the pseudo-first order rate constants ( $k_{\text{obs}}$ ) and their standard deviations.

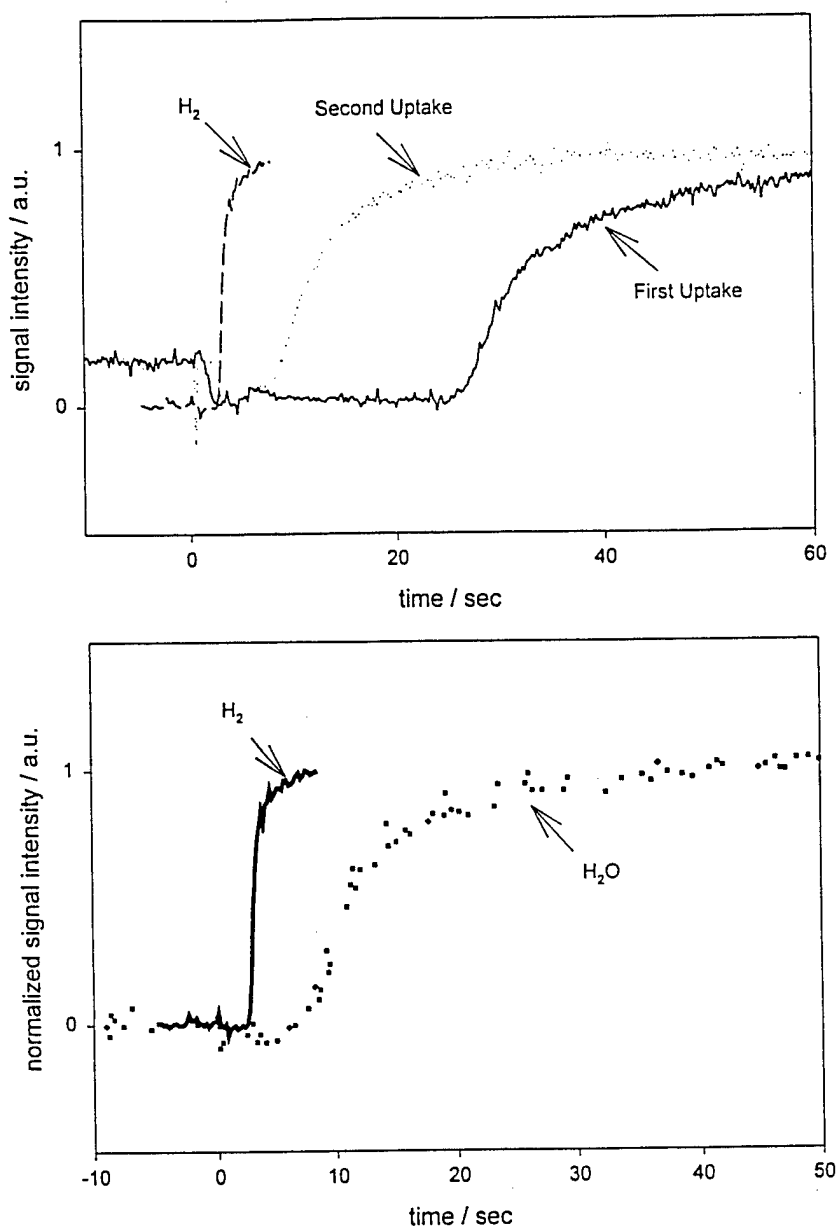
Pyrex glass for the  $\text{HCl} + \text{ClONO}_2$  reaction is indeed  $\sim 0.02$ , corroborating our earlier finding.

### **B. Uptake of Water Vapor by Alumina and Sapphire Particles**

Figure 4 shows typical breakthrough curves for the two alumina samples investigated, for experiments carried out at ambient temperature and 300 mTorr water partial pressure with a water background in the carrier gas (reference stream) of 6 mTorr. The surface area was estimated assuming spherical particles and taking into account their size distribution and the total weight of the sample. The water coverage in consecutive experiments for both types of alumina was of the order of a monolayer ( $\sim 3 \times 10^{15}$  molecule  $\text{cm}^{-2}$ ). While no difference in surface coverage between the first and consecutive experiments was observed for the sapphire particles, the  $\alpha$ -alumina sample showed a fourfold higher uptake in the first experiment after annealing to 1300 K.

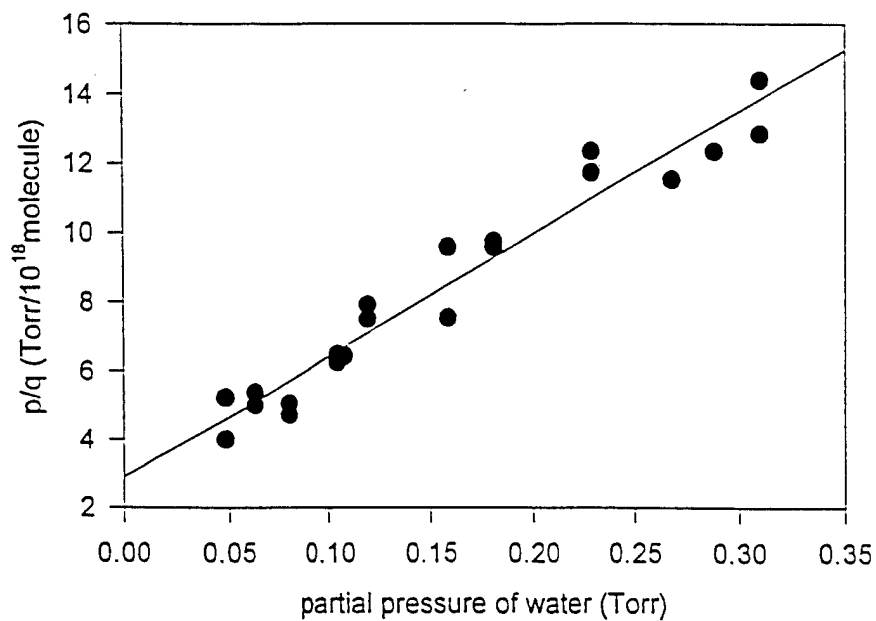
In order to further quantify the amount of water taken up by alumina particles under atmospheric conditions, we determined several adsorption isotherms. One way to represent such isotherms is to plot the partial pressure of water ( $p$ ) divided by the amount of water taken up ( $q$ ) as a function of  $p$ . Figure 5 displays such an isotherm. The linear fit is derived from the conventional Langmuir adsorption isotherm model [Ruthven, 1984], and yields a saturation limit  $q_s = 1.4 \times 10^{18}$  molecule and a Henry constant  $K_H = 1.7 \times 10^{19}$  molecule/Torr. The sample consisted of 18 mg of 105 to 200  $\mu\text{m}$  particles corresponding to a geometric surface area of approximately  $6 \text{ cm}^2$ .

Figure 6 shows a reversible uptake experiment at 300 K on sapphire (77 mg of 105 to 180  $\mu\text{m}$  particles corresponding to a geometric surface area of approximately  $22 \text{ cm}^2$ ). The partial pressure of water in the wet stream of the carrier gas (10 sccm of He) corresponds to  $p = 38.9$  ppm at a background concentration in the dry stream of  $p_0 = 10.7$  ppm. The incremental amount of adsorbed water calculated from the breakthrough curve is  $q - q_0 = 1.77 \times 10^{15}$  molecule. From  $t = 400$  s to  $t = 800$  s the sample is heated to 1300 K and  $1.18 \times 10^{15}$  molecules of water desorb. When cooling the sample back to 300 K, the signal decreases shortly before increasing to the initial steady state level again. In this process, the previously desorbed amount of water is readsorbed, as can be inferred from



**Figure 4:** Uptake of water on  $\alpha$ -alumina at 300 K and standard pressure after annealing the alumina at 1300 K. Breakthrough signals were monitored at 300 mTorr partial pressure of water and 10 sccm He carrier gas flow. Also shown is the reference experiment using  $H_2$  instead of  $H_2O$  as a probe gas.

- (a) Commercial  $\alpha$ -alumina. Particle size: 0.15 to 0.2 mm; column length: 2 cm; estimated surface area: 3.6 cm<sup>2</sup>. The first and subsequent uptakes correspond to  $5.2 \times 10^{16}$  molecules and  $1.5 \times 10^{16}$  molecules, respectively.
- (b) Sapphire. Particle size: 0.2 to 0.8 mm; column length: 5 cm; estimated surface area: 3.6 cm<sup>2</sup>. The first and subsequent uptakes are equal and correspond to  $1.9 \times 10^{16}$  molecules.



**Figure 5:** Langmuir adsorption isotherm at 300 K for Cerac alumina.  $q$  is the amount of water taken up, and  $p$  is the partial pressure of water.  $p/q$  is plotted against  $p$ . The linear fit yields a saturation limit  $q_s = 1.35 \times 10^{18}$  molecules and Henry constant  $K_H = 16.7 \times 10^{18}$  molecule Torr<sup>-1</sup>. The sample consisted of 18 mg of 105 to 200  $\mu\text{m}$  particles; estimated surface area: 5 cm<sup>2</sup>.

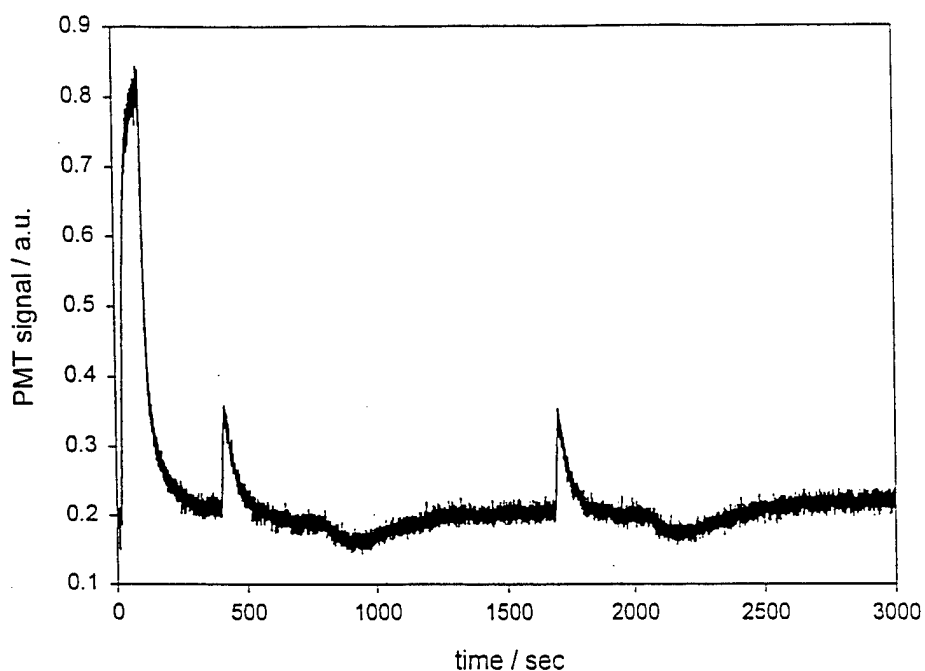


**Figure 6:** Reversible uptake experiment at 300 K on sapphire followed by two heating-cooling cycles to 1300 and 300 K, respectively. The wet and dry gas streams correspond to 38.9 and 10.7 ppm of water, respectively. In the initial uptake experiment  $1.77 \times 10^{15}$  molecules are adsorbed reversibly. The sample was heated between 400 and 800 sec and between 1700 and 2000 sec. In these heating-cooling cycles,  $1.18 \times 10^{15}$  molecules desorb and readsorb. The sample consisted of 77 mg of 105 to 180  $\mu\text{m}$  particles; estimated surface area: 22  $\text{cm}^2$ .

consecutive heating-cooling cycles. The results of similar experiments carried out down to temperatures around 240 K indicate that the alumina particles also adsorb water efficiently under stratospheric conditions.

Early reports by Steven George of the University of Colorado suggested that alumina would lose its surface hydroxyl groups when heated above about 600 °C, and that water vapor would not react with the surface to regenerate the hydroxyl groups below that temperature. The implication was that alumina particles in the stratosphere would not adsorb water, because they are formed in the SRM's at relatively high temperatures. We countered that the particles would recover their surface OH groups by reacting not with water vapor, but with OH or HO<sub>2</sub> radicals.

As described above, our measurements indicate, however, that even sapphire particles—that are characterized by having an extremely inert surface—adsorb monolayer quantities of water after being heated above 600 °C. The measurements were carried out under atmospheric conditions of temperature and humidity. Thus, the mechanism we had proposed for the chlorine activation reaction appears to be applicable, the adsorbed water providing the means for the ionic aqueous-type reaction to take place. Subsequent work by Steven George's group indicated that the OH groups would not be permanently lost as readily as initially envisioned; furthermore, it was realized that even dehydroxylated alumina adsorbs water. Hence, some of the experiments we had proposed to carry out involving reaction of OH and HO<sub>2</sub> radicals with "clean" alumina surfaces turned out to be unnecessary. The water uptake experiments in S. George's group are complementary to our own: their measurements were carried out under high vacuum conditions, so that only the chemisorbed water is retained, except at temperatures well below those prevailing in the stratosphere. Our measurements are designed to monitor not only chemisorbed but also physisorbed water, which is the form that enables the ionic chlorine activation reaction to take place.

Our water uptake experiments did reveal differences in the surface activity of sapphire compared to conventional alumina. The uptake by sapphire is reversible, involving only physical adsorption: the water taken up was released by flowing dry carrier gas at room temperature or below. In contrast, the conventional alumina surface

chemisorbs some fraction of the water, and at room temperature it only loses upon exposure to dry carrier gas the portion that is physisorbed. Therefore, we infer that alumina particles emitted by SRM's will be catalytically active in the stratosphere, because they will be covered by adsorbed water. Surface imperfections and impurities such as chloride or nitrate groups may modify the extent of chemisorbed water, but physisorbed water will be surely present, enabling the chlorine activation reaction to take place as predicted.

## CONCLUSIONS

We have measured the reaction probabilities for the reaction of  $\text{ClONO}_2$  with  $\text{HCl}$  on laboratory alumina, on alumina particles emitted by SRMs, and on glass surfaces, under temperature, water and reactant partial pressure conditions similar to those encountered at mid-latitudes in the lower stratosphere. On all these surfaces the reaction probability value we measured is  $\sim 0.02$ , whereas the value on ice surfaces is larger than 0.2. The reaction mechanism on glass and alumina appears to depend more on the presence of adsorbed water layers than on the presence of active sites or the detailed nature of the refractory oxide surface itself. We have also measured the amount of water taken up by the alumina and glass surfaces, establishing that water layers indeed cover these surfaces under stratospheric conditions.

Our results suggest that on a global scale, the ozone depletion effect of the particles emitted by SRMs is comparable to the effect of the chlorine emissions from the SRMs. Overall, the global effect of SRMs currently in use is small compared to the effect of industrial chlorofluorocarbons and Halons.

**Acknowledgment** We thank Dr. R. R. Bennet of Thiokol Propulsion Inc. for providing the SRM dust and Dr. V. Lang of the Aerospace Corporation for providing the SRM slack.

## REFERENCES

- Beiting, E.J. *Aerospace Report No. Tr-95(5231)-8* 1995, Aerospace Corporation.
- Brady, B. B.; Martin, L.R.; Lang, V.I. *J. Spacecrafts & Rockets*, 1997, 34(6), 774.
- Brownlee, D. E.; Ferry, G.V.; Tomandl, D. *Science*, 1976, 191, 1270.
- Cofer, W.R. III; Winstaed, E.L.; Key, L.E. *J. Propulsion* 1989, 5, 674.
- Denison, M. R.; Lamb, J.J.; Bjorndahl, W.D.; Wong, E.Y.; Lohn, P.D. *J.Spacecraft & Rockets*, 1994, 31, 435.
- Hanson, D.R.; Ravishankara, A.R. *J. Geophys. Res.* 1991, 96, 5081.
- Jackman, C.H.; Considine, D.B.; Fleming, E.L. *Geophys. Res. Lett.* 1998, 25, 907.
- Jones, A.E.; Bekki, S.; Pyle, J.A. *J. Geophys. Res.* 1995, 100, 16651.
- Keyser, L.F.; Moore, S.B.; Leu M.-L. *J. Phys. Chem.* 1991, 95, 5496.
- Molina, L.T.; Spencer, J.E.; Molina, M.J. *Chem. Phys. Lett.* 1977, 45, 158. .
- Molina, M. J.; T.-L. Tso, T.-L.; Molina, L.T.; Wang, F.C.-Y. *Science*, 1987, 238, 1253.
- Molina, M.J.; Molina, L.T.; Zhang, R.; Meads, R.F.; Spencer, D.D. *Geophys. Res. Lett.* 1997, 24, 1619.
- Prather, M. J.; Garcia, M.M.; Douglass, A.R.; Jackman, C.H.; Ko, M.K.W.; Sze, N.D. *J. Geophys. Res.*, 1990, 95, 18583.
- Ross, M. N.; Benbrook, J.R.; Sheldon, W.R.; Zittel, P.F.; McKenzie, D.L. *Nature*, 1997, 390, 62.
- Ross, M.N., Ballenthin, J.O.; Gosselin, R.B.; Meads, R.F.; Zittel, P.F., Benbrook, J.R.; Sheldon, W.R. *Geophys. Res. Lett.* 1997, 24, 1755.
- Ruthven, D.M., *Principles of Adsorption and Adsorption Processes*, John Wiley and Sons, 1984.
- WMO, *Scientific Assessment of Ozone Depletion: 1994, World Meteorological Organization, Global Ozone Research and Monitoring Project, Report No. 37*, 1995.
- Zasytkin, A.Y.; Grigor'eva, V.M.; Korchak, V.N.; Gershenson, Y.M. *Kinetics and Catalysis*, 1997, 38, 842.
- Zhang, R.; Molina, L.T.; Molina, M.J. (1998). *Rev. Sci. Instrum.* 1998, 69, 1.
- Zolensky, M. E.; McKay, D.S.; Kaczor, L.A. *J. Geophys. Res.*, 1989, 94, 1047.

## APPENDIX

### Electrostatic Ion Guide in Chemical Ionization Mass Spectrometry

In this report we describe the development of an electrostatic ion guide for use in chemical ionization mass spectrometry. Electrostatic ion guides have been suggested as efficient ion transport devices, and have been used for many applications. A schematic diagram of the experimental apparatus used in the present study is shown in Figure A1:

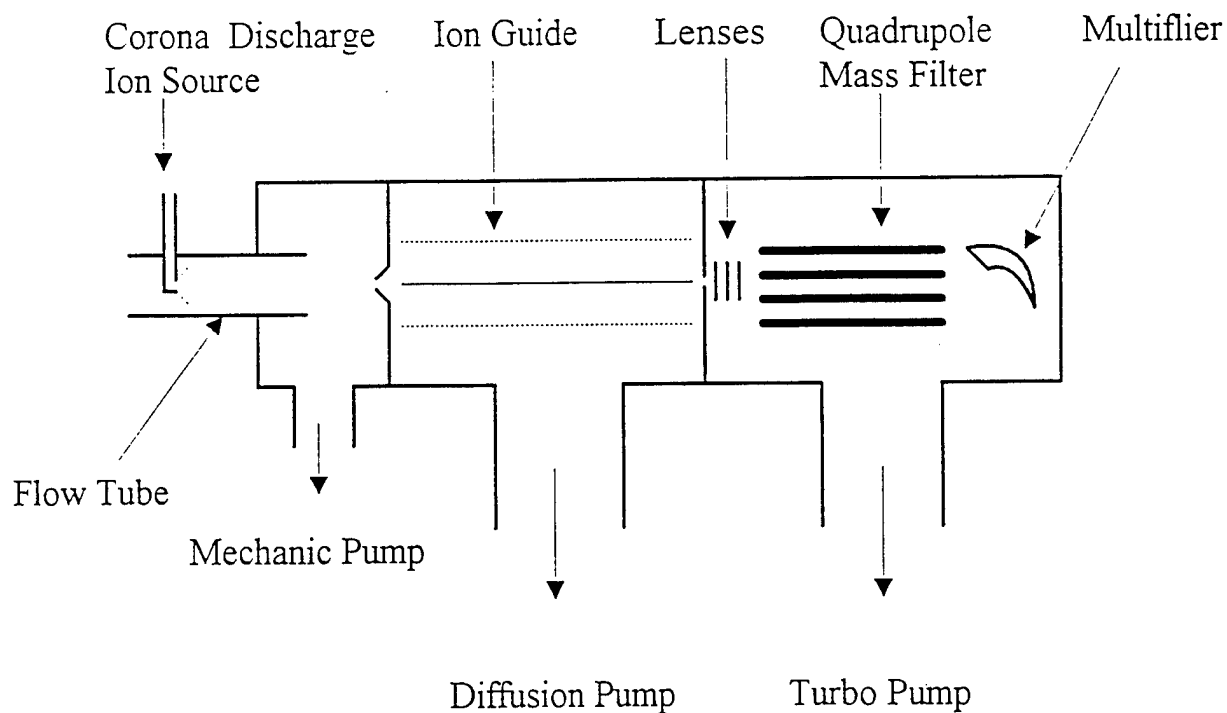


**Fig. 1A:** Schematic representation of the experimental apparatus.

The ion guide consists of an outer cylinder and a central wire. The cylinder, 11.4 cm long and 3.8 cm I.D., is made of stainless steel mesh with 0.02-mm diameter wire and 16x16 mesh plain. The central wire consists of 0.07-mm diameter nichrome wire which is mounted axially down the length of the mesh cylinder, supported by thin plastic strings attached to each end of the cylinder. Ionization and ion-molecule reactions take place in a flow tube in the pressure range from 0.5 to 10 Torr, with a mean flow velocity between 500 and 3000 cm s<sup>-1</sup>. Helium or nitrogen is used as the carrier gas in the flow reactor. Positive or negative reagent ions are created by negative corona discharge at 5 KV. Only a small fraction of the gases in the flow tube is drawn into a vacuum chamber through a sampling aperture of 1.5 mm diameter; an expanding beam is generated behind this orifice. The ion guide is placed between two charged apertures, one in front of the ion source and the other leading to the quadrupole mass analyzer. The use of a mesh cylinder permits efficient removal of neutral molecules by a diffusion pump, but restricts ions to a spiral motion along the guide, owing to the existence of an electric field between the two charged electrodes. Also, since the ion guide transports ions injected off the central axis, a precise alignment of the guide with the apertures is not necessary. The pressure in the vacuum chamber that houses the ion guide is in the range from 10<sup>-7</sup> to 10<sup>-5</sup> Torr. The size of the second aperture leading the ions into the mass spectrometer chamber was varied from 10  $\mu$ m to 5 mm in this study. The ions are focused with a set of electrostatic lenses before being mass filtered.

We have performed numerous ion trajectory simulations for conditions relevant to our experimental configurations and with various parameters for the injected ions and the guide using SIMION 3D Version 6.0. The results show that ions are transported in bound spiral orbits through the electric field produced by a potential difference between the two concentric electrodes. In all cases, the ions execute similar trajectories, except for the orbital radius about the central axis. The ion guide appears capable of transmitting ions of various initial kinetic energies, which are initially displaced from the z-axis and have trajectories diverging from the z axis.

To evaluate experimentally the ion transmission efficiency through the ion guide, a picoammeter (Keithley Model 485) was employed to measure ion currents on the

entrance and exit aperture plates, the outer cylinder, and the central wire, using  $\text{SF}_6^+$  ions. To account for the total ion current intercepted by the outer cylinder, the mesh cylinder was covered by a thin aluminum sheet of similar dimensions to prevent ions leaking through the mesh grid. Ions transmitted through the guide produced a current on the exit plate, which had an aperture of only 10  $\mu\text{m}$  diameter to minimize the number of ions passing through the orifice. Results of the current measurements show that the ion current transmitted through the guide increased markedly when appropriate voltages were applied. An ion transmission efficiency of 0.65 was derived, with an estimated uncertainty of  $\sim 20\%$ . The fraction of ions lost due to collisions with the central wire, on the other hand, was negligible ( $<2\%$ ).

The efficient separation of ions and neutral molecules is a major advantage of the ion guide described here. The use of a mesh cylinder, which retains practically all electrostatic properties of a solid cylindrical conductor, allows preferential removal of neutral molecules, while ions are transported through the guide. In general, the maximum concentration of a gas flow passing through a circular aperture occurs on axis; it is determined by the cosine law of emission, and hence the molecular density decreases rapidly away from the source (it is inversely proportional to the distance square). Hence, under our laboratory conditions, a decrease of more than two orders of magnitude in the density of neutral beam molecules is expected at the exit end of an  $\sim 11$  cm long ion guide. Using a 0.5 mm diameter aperture at the exit plate, a nearly 50-fold pressure rise in the ion guide chamber results in only a two-fold pressure increase in the next stage, owing largely to the consequent higher pumping conductance and reduced beam intensity. This is in contrast to a pressure rise of more than an order of magnitude experienced by a molecular beam system of similar configuration having, however, a distance of only  $\sim 5$  cm between the two apertures.

In summary, an electrostatic ion guide has been successfully developed for chemical ionization mass spectrometry. A significant advantage of this system is its simplicity and ability to separate ions from neutral molecules, providing a means to significantly improve the detection sensitivity.